

Supporting Information

Understanding the interfacial charge transfer in CVD grown $\text{Bi}_2\text{O}_2\text{Se}/\text{CsPbBr}_3$ nanocrystals heterostructure and its exploitation in superior photodetection: Experiment vs. Theory

Md Tarik Hossain¹, Mandira Das¹, Joydip Ghosh¹, Subhradip Ghosh¹, and P. K.

Giri^{1, 2*}

¹Department of Physics, Indian Institute of Technology Guwahati, Guwahati - 781039, India

²Centre for Nanotechnology, Indian Institute of Technology Guwahati, Guwahati - 781039,
India

Table S1: Details of the fitting parameters of time-resolved PL decay profiles for CsPbBr_3 NCs and $\text{Bi}_2\text{O}_2\text{Se}/\text{CsPbBr}_3$ heterostructure.

Sample	τ_1 (ns)	A_1	τ_2 (ns)	A_2	τ_{ave} (ns)
CsPbBr_3	4.55	2916	8.65	924	5.54
$\text{Bi}_2\text{O}_2\text{Se}/\text{CsPbBr}_3$	1.60	2828	4.55	2781	3.06

* Corresponding authors, email giri@iitg.ac.in (PKG),

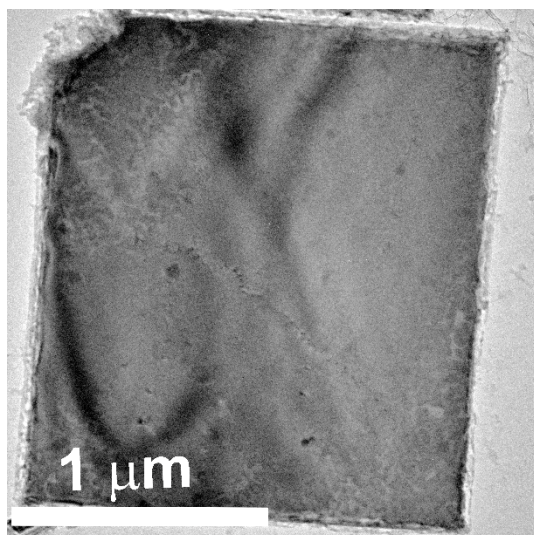


Fig. S1: TEM image of a $\text{Bi}_2\text{O}_2\text{Se}$ flake.

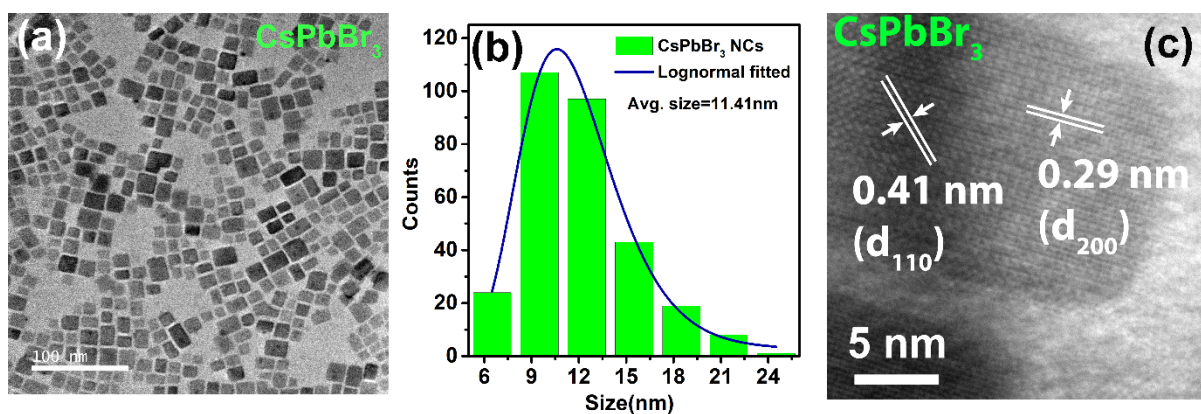


Fig. S2: (a) TEM image of as-synthesized CsPbBr_3 NCs. (b) A histogram of the size distributions of CsPbBr_3 NCs. The solid line shows the corresponding log-normal fitting to determine the average size of the NCs. (c) HRTEM image of a single CsPbBr_3 NC.

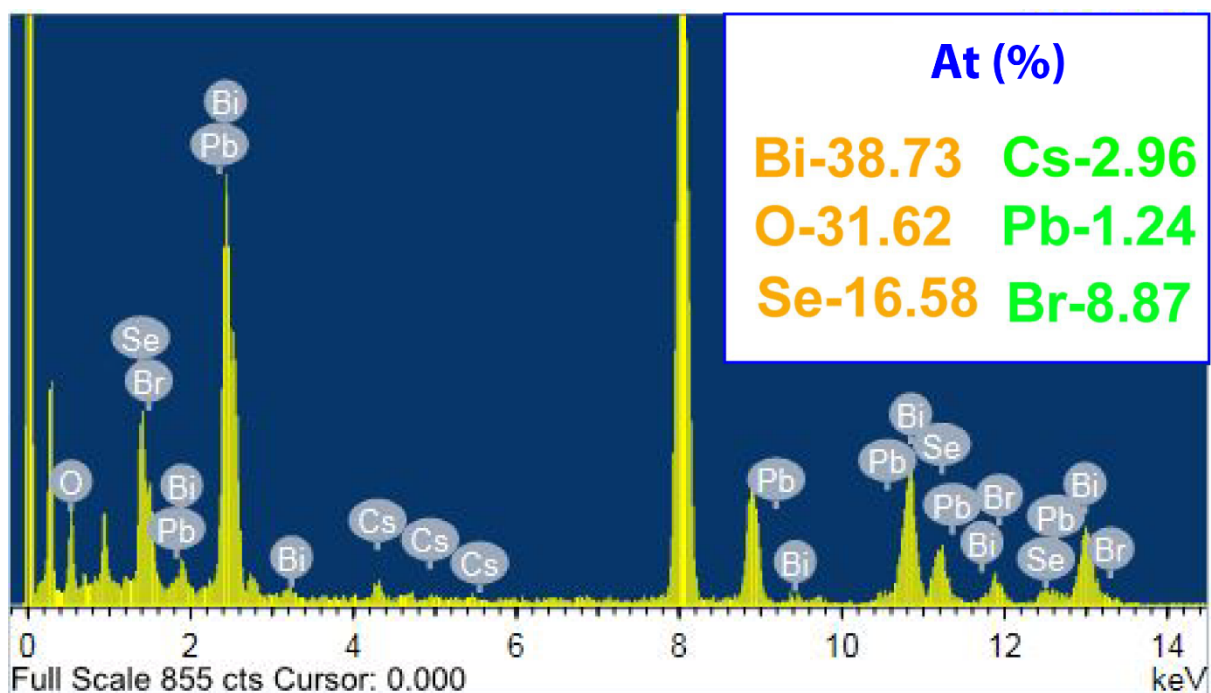


Fig. S3: EDX spectrum of $\text{Bi}_2\text{O}_2\text{Se}/\text{CsPbBr}_3$ NCs heterostructure.

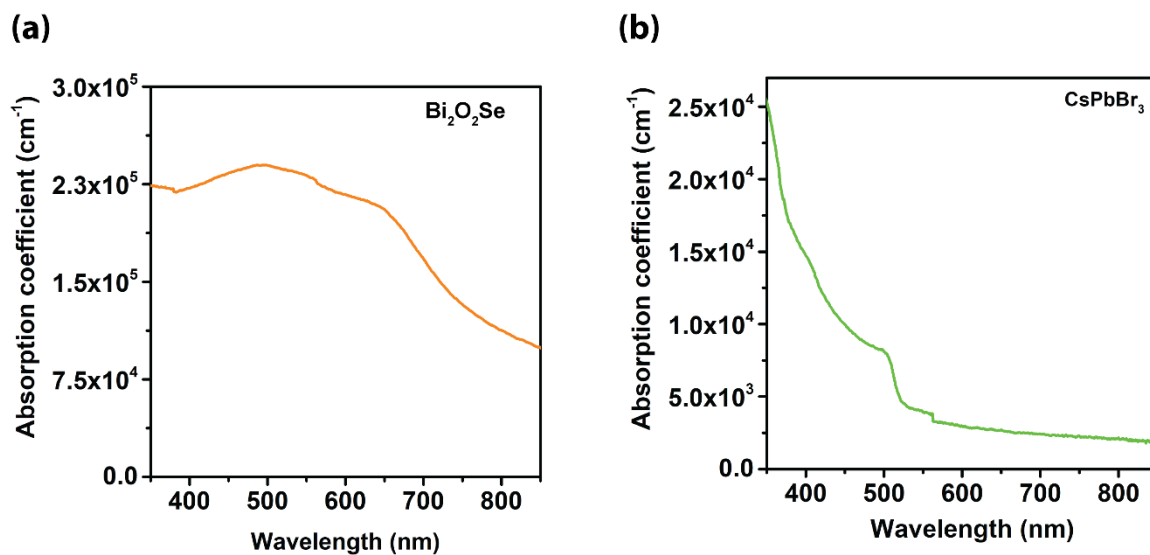


Fig. S4: Absorption coefficient of (a) as-grown $\text{Bi}_2\text{O}_2\text{Se}$ flakes (b) CsPbBr_3 NCs.

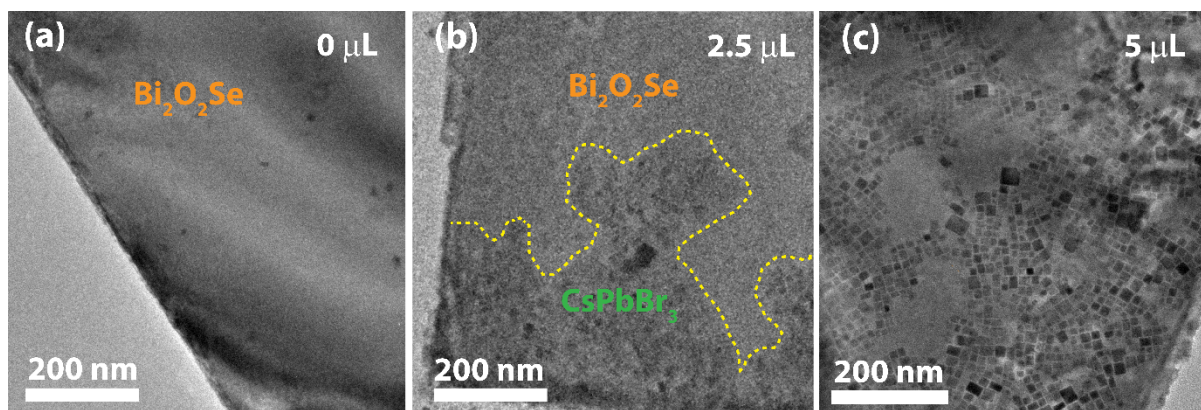


Fig. S5: TEM image of Bi₂O₂Se flakes with (a) 0 μ L (b) 2.5 μ L (c) 5.0 μ L of CsPbBr₃ NCs.

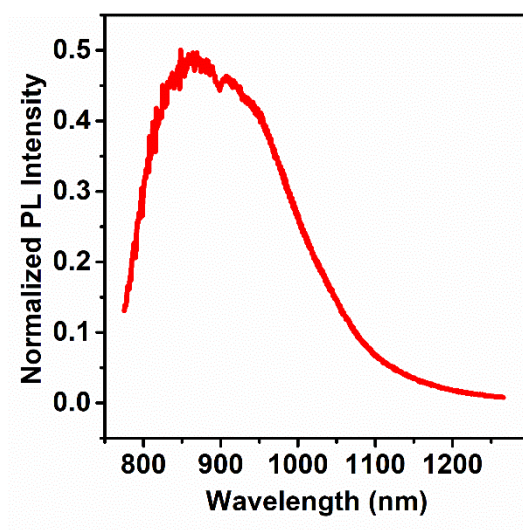


Fig. S6: Near-infrared photoluminescence emission spectrum of pristine Bi₂O₂Se flakes at room temperature.

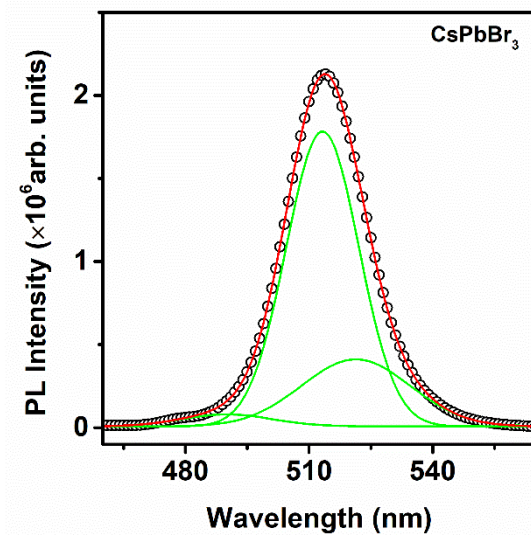


Fig. S7: Steady-state photoluminescence emission spectrum of pristine CsPbBr₃ at room temperature. Symbols represent the experimental data, and the solid line shows the Gaussian fitting.

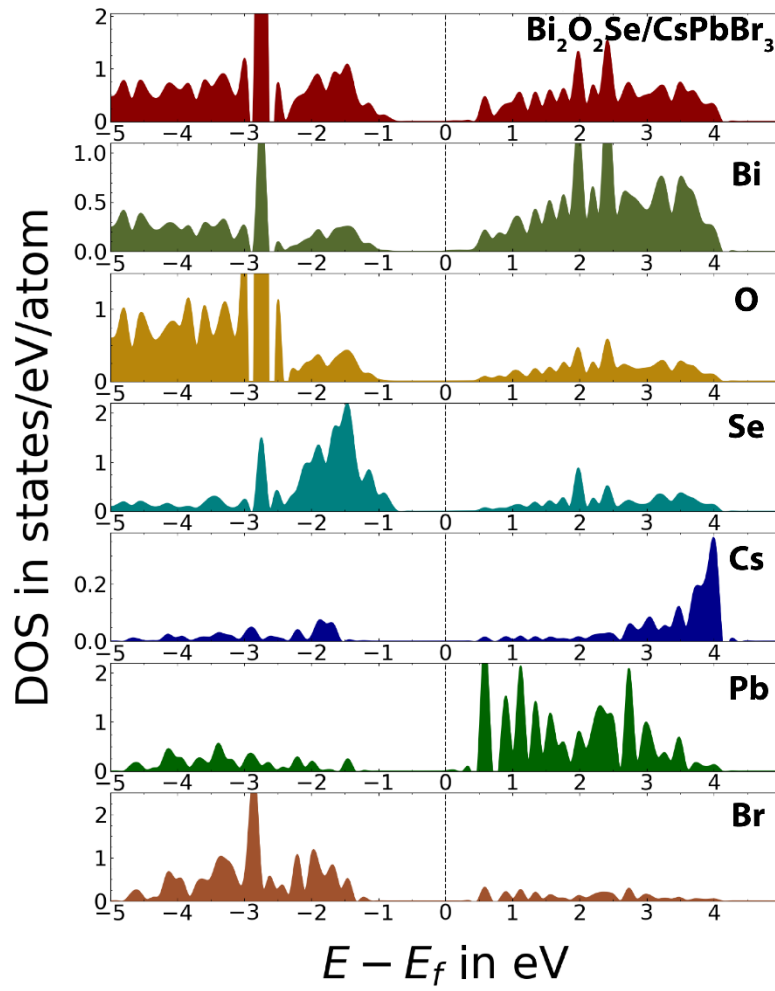


Fig. S8: TDOS and PDOS of bilayer $\text{Bi}_2\text{O}_2\text{Se}/\text{CsPbBr}_3$ NC heterostructure.

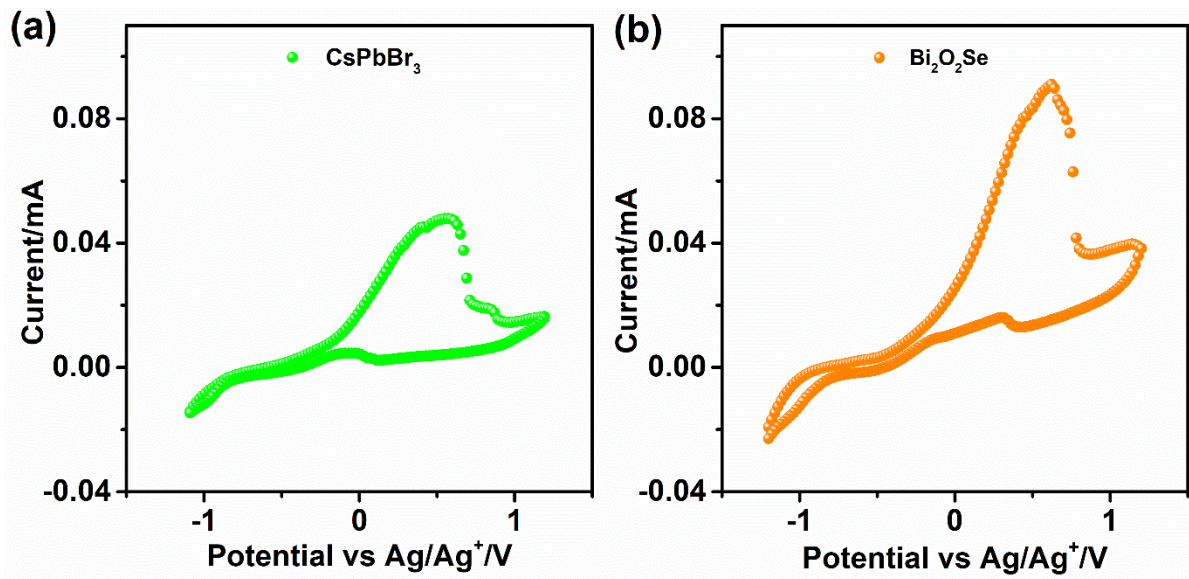


Fig. S9: Cyclic voltammetry spectra of pristine (a) CsPbBr₃ NCs and (b) 2D Bi₂O₂Se.

Cyclic voltammetry (CV) analysis:

CV measurement was performed to derive the band positions of Bi₂O₂Se and CsPbBr₃. The band positions were obtained following the equations,[1]

$$E_{VB} = - (E_{ox} + 4.71) \text{ eV}$$

$$E_{CB} = - (E_{red} + 4.71) \text{ eV}$$

$$\text{Electrochemical band gap} = E_{CB} - E_{VB}$$

Bi₂O₂Se:

$$E_{VB} = - (E_{ox} + 4.71) \text{ eV} = - (0.629 + 4.71) \text{ eV} = - 5.339 \text{ eV}$$

$$E_{CB} = - (E_{red} + 4.71) \text{ eV} = - (- 0.405 + 4.71) \text{ eV} = - 4.305 \text{ eV}$$

$$\text{Electrochemical band gap} = (- 4.305 - (-5.339)) \text{ eV} = 1.034 \text{ eV}$$

CsPbBr₃:

$$E_{VB} = - (E_{ox} + 4.71) \text{ eV} = -(1.08 + 4.71) \text{ eV} = -5.79 \text{ eV}$$

$$E_{CB} = - (E_{red} + 4.71) \text{ eV} = -(-1.01 + 4.71) \text{ eV} = - 3.7 \text{ eV}$$

$$\text{Electrochemical band gap} = (- 3.7 - (- 5.8)) \text{ eV} = 2.1 \text{ eV}$$

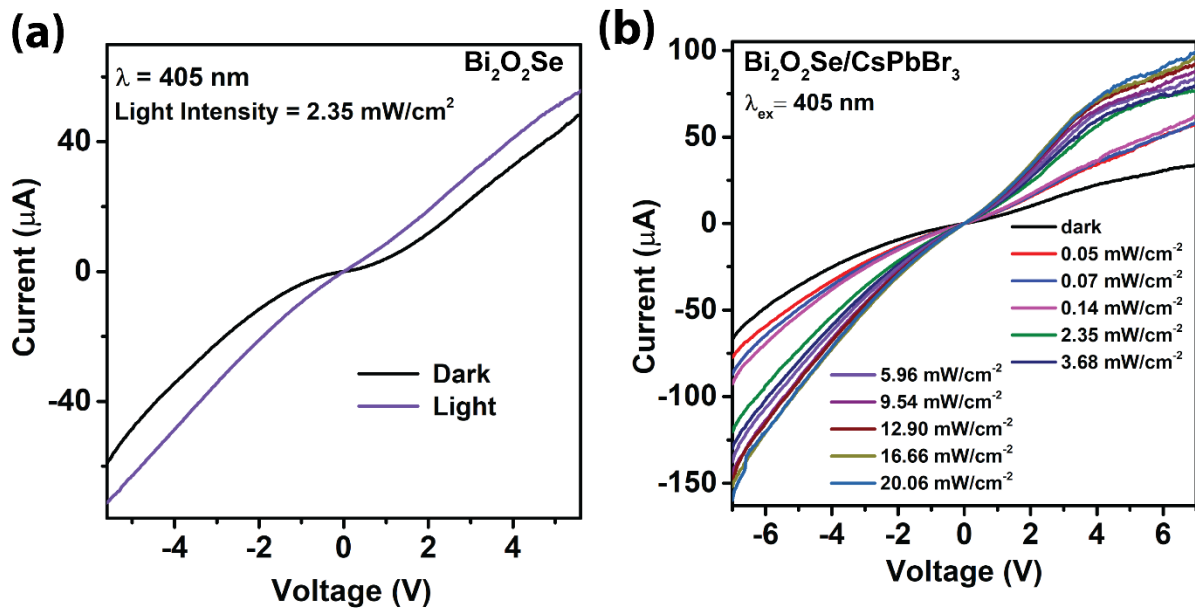


Fig. S10: (a) IV characteristics of Bi₂O₂Se photodetector under dark and light illumination. (b) Dark and photo-IV characteristics of Bi₂O₂Se/CsPbBr₃ NCs heterostructure photodetector with different excitation intensity.

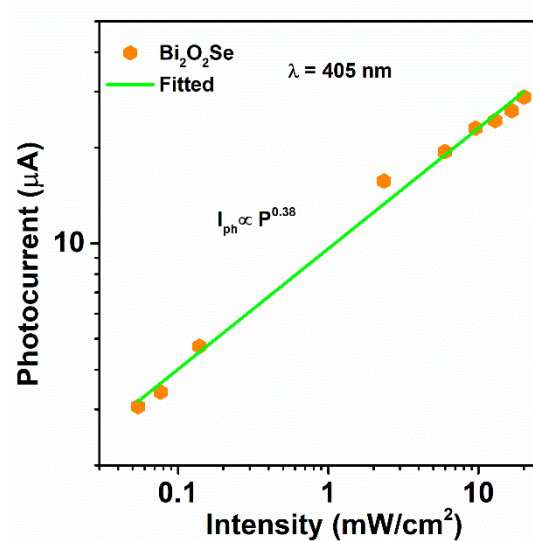


Fig. S11: Power-law fitting to the illumination power dependence of photocurrent for pristine Bi₂O₂Se device.

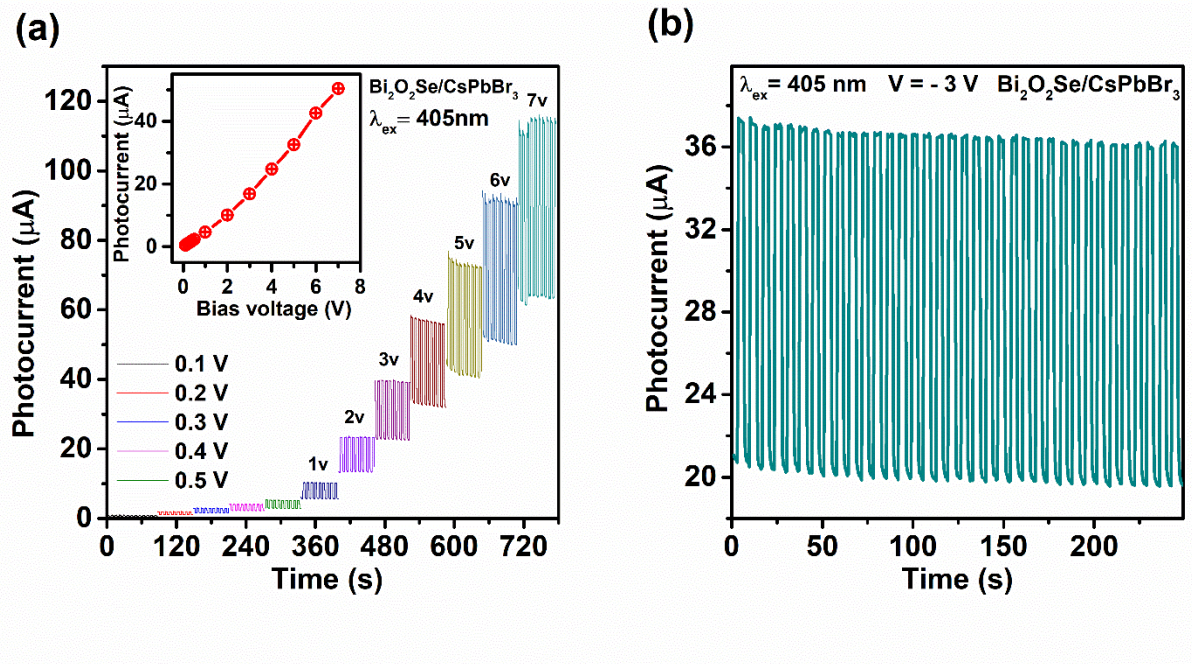


Fig. S12: (a) Photocurrent response under different bias voltages in $\text{Bi}_2\text{O}_2\text{Se}/\text{CsPbBr}_3$ NCs heterostructure photodetector. Inset depicts the nonlinear increase in photocurrent with the bias voltage. (d) Stability of photocurrent response under prolonged exposure to light pulses.

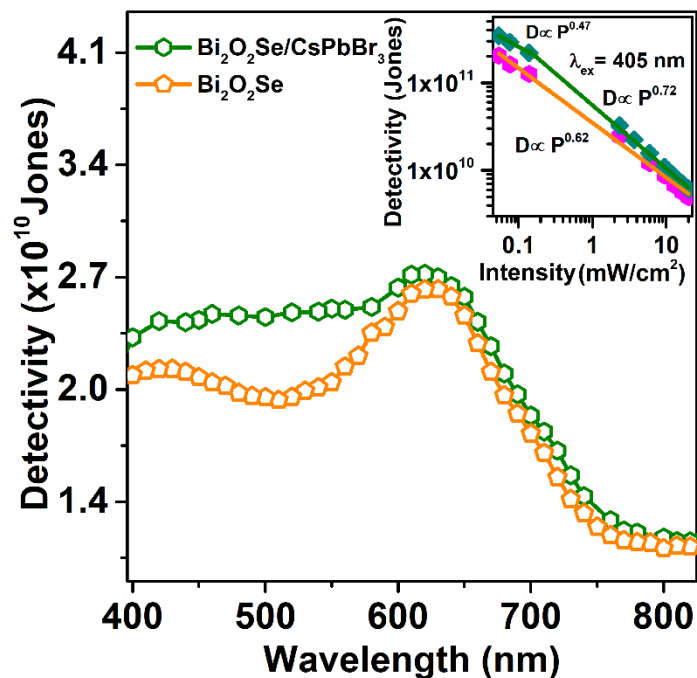


Fig. S13: Detectivity of pristine semiconducting $\text{Bi}_2\text{O}_2\text{Se}$ and $\text{Bi}_2\text{O}_2\text{Se}/\text{CsPbBr}_3$ NCs heterostructure. The inset shows the respective excitation intensity-dependent detectivity at 405 nm.

Reference

1. Barman, M.K., et al., *An efficient charge separation and photocurrent generation in the carbon dot–zinc oxide nanoparticle composite*. *Nanoscale*, 2017. **9**(20): p. 6791-6799.